

Introduction to Magnetohydrodynamic Modeling of the Magnetosphere

M. Wiltberger
NCAR/HAO

Outline

- Brief history of global modeling
- Numerical Issues related to MHD Modeling
 - Form of the Equations
 - Computational Methods
 - Parallel Computing
- Global Magnetospheric Modeling Issues
 - Grids and Boundary Conditions
 - MI Coupling
- Validation
- Conclusions and Future Directions

A Brief History of Global MHD Simulations

- 1978 – First 2D simulations by Leboeuf et al.
- Early 80s – First 3D simulations by Brecht, Lyon, Wu and Ogino
- Late 80s – Model refinements including FACs, ionospheres, higher resolution
- 90s – ISTP integrates theory and modeling with spacecraft missions and comparisons with *in situ* space and ground observations begun
- Today – Global modeling has become integrated part of many experimental studies and we've begun linking models of different regions together

Ideal MHD Equations

Non Conservative Formulation

$$\frac{\partial \rho}{\partial t} + \nabla \cdot (\rho \vec{u}) = 0$$

$$\rho \frac{\partial \vec{u}}{\partial t} + \rho (\vec{u} \cdot \nabla) \vec{u} + \nabla \left(p + \frac{B^2}{8\pi} \right) + (\vec{B} \cdot \nabla) \vec{B} = 0$$

$$\frac{\partial \vec{B}}{\partial t} + \nabla \times (\vec{u} \times \vec{B}) = 0$$

$$\frac{d}{dt} \left(\frac{p}{\rho^\gamma} \right) = 0$$

$$\nabla \cdot \vec{B} = 0$$

- No strict numerical conservation of energy and momentum
- Various numerical issues
 - Errors in propagating strong shocks
 - Errors in RH Conditions
 - Incorrect shock speeds

Ideal MHD Equations

Full Conservative Formulation

$$\frac{\partial \rho}{\partial t} + \nabla \cdot [\rho \vec{u}] = 0$$

$$\frac{\partial (\rho \vec{u})}{\partial t} + \nabla \cdot \left[\rho \vec{u} \vec{u} + \left(p + \frac{B^2}{8\pi} \right) \vec{I} + \frac{1}{4\pi} \vec{B} \vec{B} \right] = 0$$

$$\frac{\partial \vec{B}}{\partial t} + \nabla \cdot [\vec{u} \vec{B} - \vec{B} \vec{u}] = 0$$

$$\frac{\partial (\rho E)}{\partial t} + \nabla \cdot \left[\vec{u} \left(\rho E + p + \frac{B^2}{8\pi} \right) - \vec{B} (\vec{u} \cdot \vec{B}) \right] = 0$$

$$\nabla \cdot \vec{B} = 0$$

$$p = (\gamma - 1) \left[E - \frac{1}{2} \rho u^2 - \frac{1}{2} B^2 \right]$$

- Strict numerical conservation of mass, momentum and energy
- Numerical difficulties in low \mathbb{W} regions
 - negative pressures possible because p becomes difference of two large numbers

Ideal MHD Equations

Gas Conservative Formulation

$$\frac{\partial \rho}{\partial t} + \nabla \cdot [\rho \vec{u}] = 0$$

$$\frac{\partial (\rho \vec{u})}{\partial t} + \nabla \cdot \left[\rho \vec{u} \vec{u} + \left(p + \frac{B^2}{8\pi} \right) \vec{I} + \frac{1}{4\pi} \vec{B} \vec{B} \right] = 0$$

$$\frac{\partial \vec{B}}{\partial t} + \nabla \cdot [\vec{u} \vec{B} - \vec{B} \vec{u}] = 0$$

$$\frac{\partial (E_p)}{\partial t} + \nabla \cdot \left[\vec{u} \left(\frac{\rho u^2}{2} + \frac{\gamma}{\gamma-1} p \right) \right] + u \cdot \nabla \cdot \left[\frac{B^2}{8\pi} \vec{I} - \frac{\vec{B} \vec{B}}{4\pi} \right] = 0$$

$$\nabla \cdot \vec{B} = 0$$

$$p = (\gamma - 1) \left[E_p - \frac{1}{2} \rho u^2 \right]$$

- Strict numerical conservation of mass, momentum and plasma energy
 - Final term in Energy equation is $\vec{j} \cdot \vec{E}$ dotted with velocity
 - no strict conservation of total energy
- No difficulties in low \mathbb{W} regions

Time Differencing

- Explicit time differences
 - Predictor – Corrector (2nd order accurate)

$$U^{n+\frac{1}{2}} = U^n - \frac{1}{2} \Delta t \nabla \cdot F(U^n)$$

$$U^{n+1} = U^n - \Delta t \nabla \cdot F(U^{n+\frac{1}{2}})$$

- Leap Frog Scheme (2nd order accurate)

$$U^{n+1} = U^{n-1} - 2\Delta t \nabla \cdot F(U^n, U^{n-1})$$

- Stability Criterion (CFL Condition)

$$\Delta t_{\max} \leq \frac{\min(\Delta x)}{v}$$

- Implicit Schemes generally not used because solution of large linear systems becomes too expensive

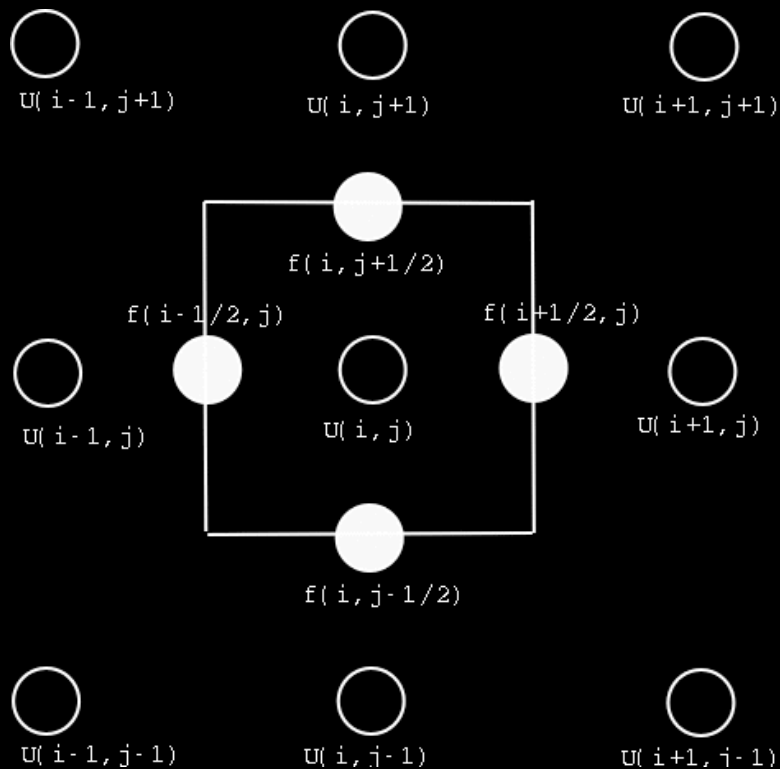
MHD Numerics

- Need a method to solve the conservative formulation of the MHD equations which maintains the conservation properties
- For this discussion we'll consider the linear advection equation

$$\frac{\partial U}{\partial t} + \nabla \cdot F(U) = 0$$

$$\frac{\partial U}{\partial t} + v \frac{\partial U}{\partial x} = 0$$

Spatial Discretization



Conservative Finite Difference Scheme

- State variables are cell centered quantities and we discretize our model equation with numerical fluxes through the cell interfaces

$$\frac{dU}{dt} = -(f_{i+\frac{1}{2}}(U) - f_{i-\frac{1}{2}}(U)) / \Delta x$$

- Scheme is conservative because

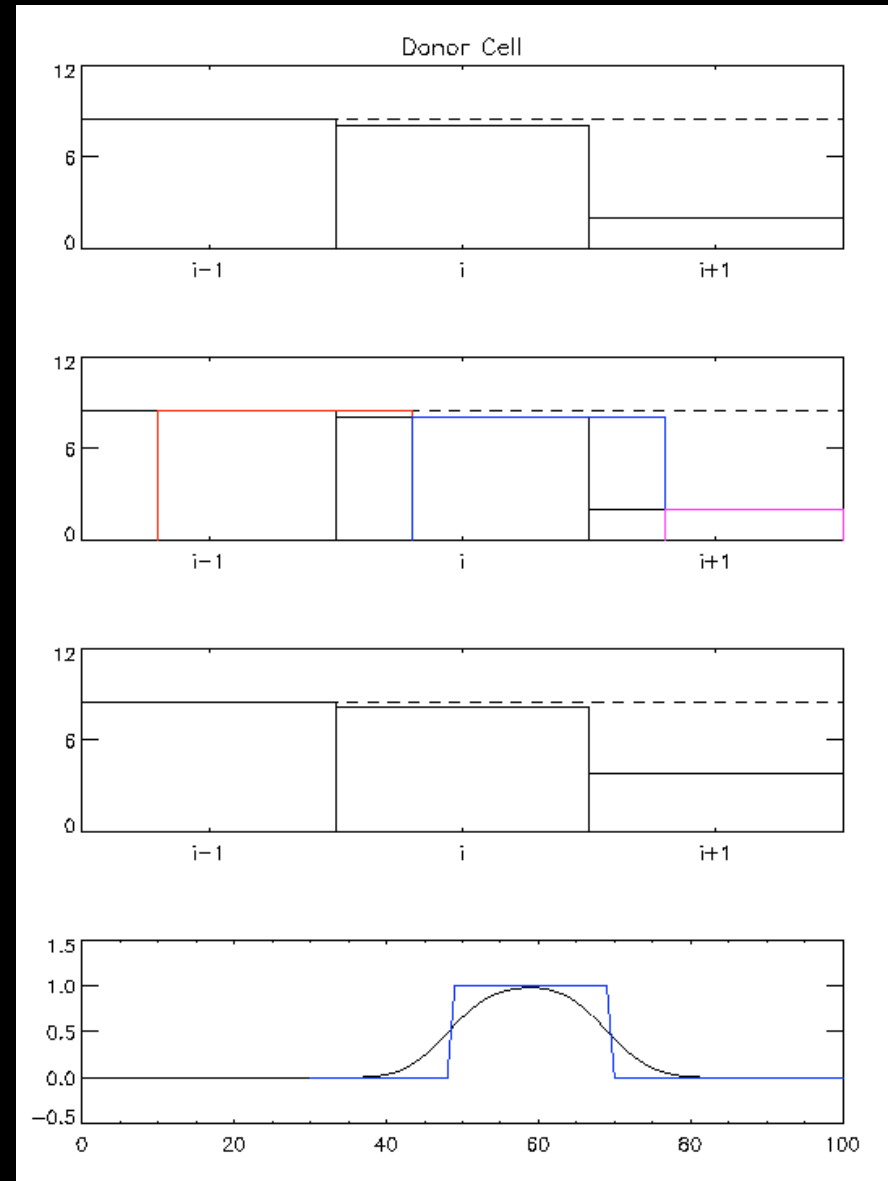
$$\frac{\partial}{\partial t} \iiint_V U dV = \iint_S F ds$$

Donor Cell

- A simple first order algorithm

$$\begin{aligned}u_i^{n+1} &= u_i^n + \frac{v\Delta t}{\Delta x} (F_{i-1/2} - F_{i+1/2}) \\ &= u_i^n + \frac{v\Delta t}{\Delta x} (u_{i-1}^n - u_i^n)\end{aligned}$$

- Maintains monotonic solution
- Linear advection problem clearly shows diffusive character

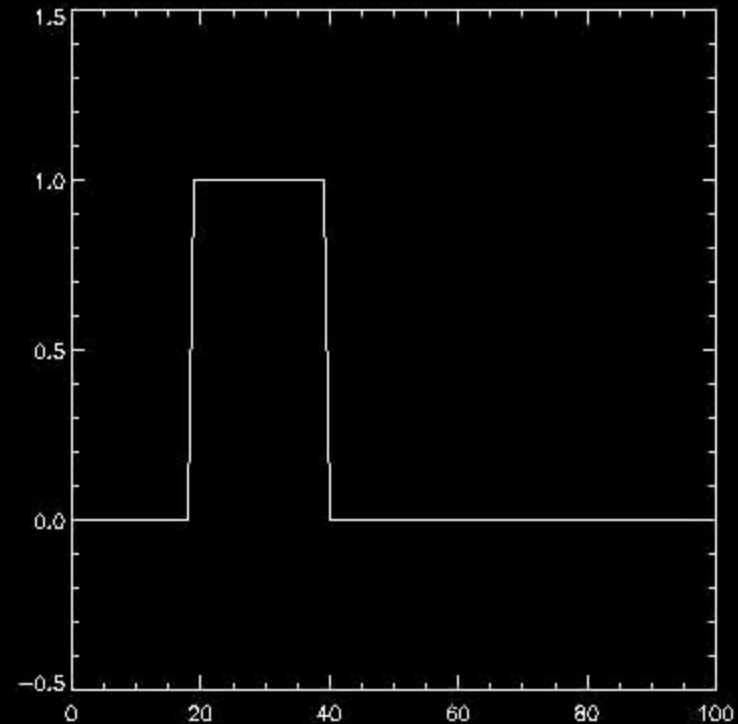


Donor Cell

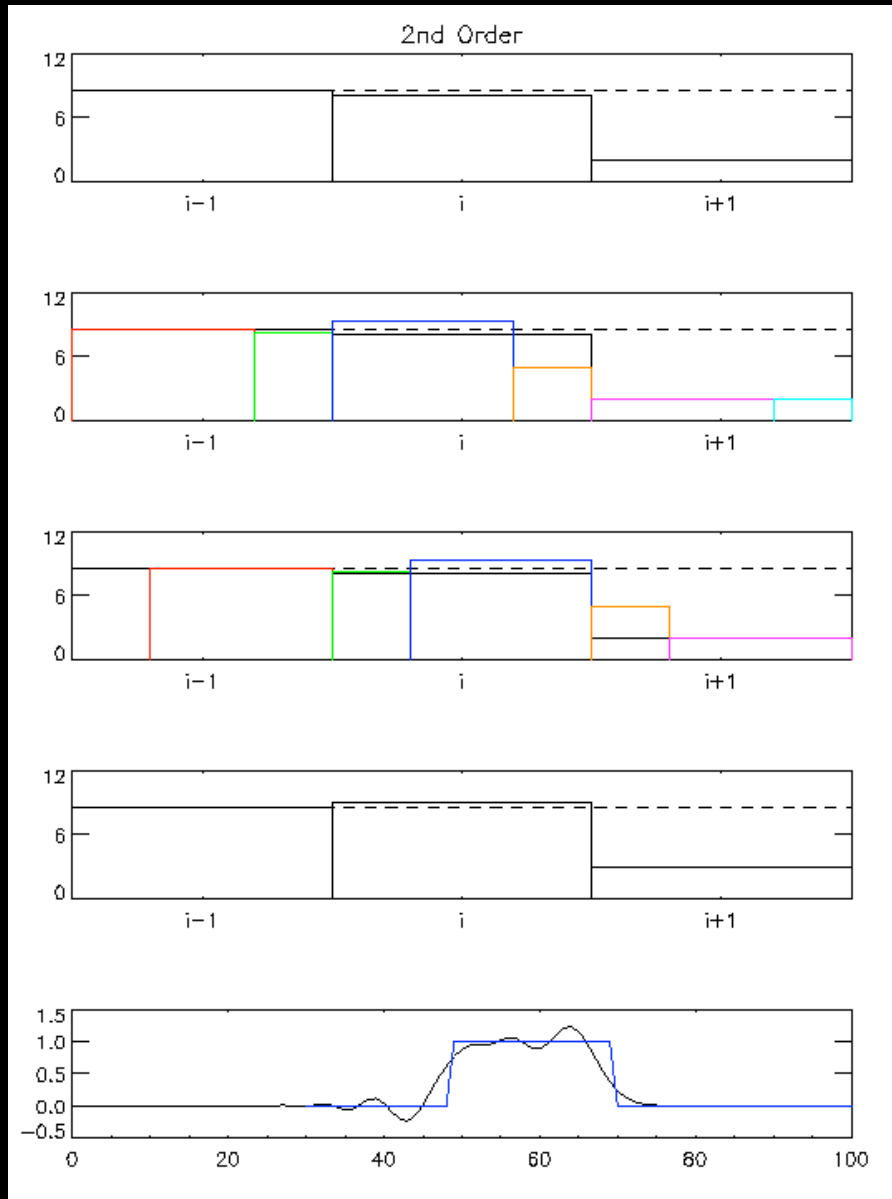
- A simple first order algorithm

$$\begin{aligned}u_i^{n+1} &= u_i^n + \frac{v\Delta t}{\Delta x} (F_{i-1/2} - F_{i+1/2}) \\ &= u_i^n + \frac{v\Delta t}{\Delta x} (u_{i-1}^n - u_i^n)\end{aligned}$$

- Maintains monotonic solution
- Linear advection problem clearly shows diffusive character



Second Order

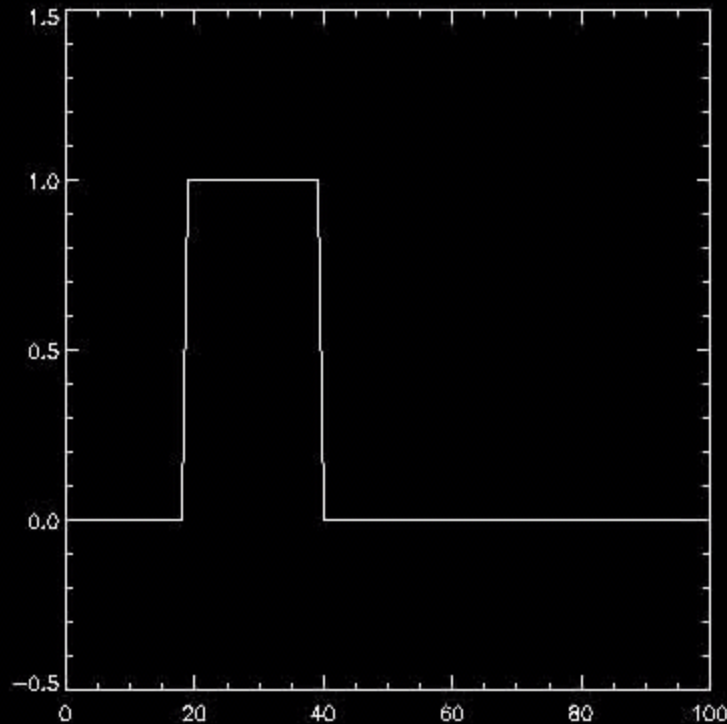


- A simple second order algorithm

$$\begin{aligned}
 u_i^{n+1} &= u_i^n + \frac{v\Delta t}{\Delta x} (F_{i-1/2} - F_{i+1/2}) \\
 &= u_i^n + \frac{v\Delta t}{\Delta x} \left(\frac{1}{2} (u_{i-1}^n - u_i^n) - \frac{1}{2} (u_i^n - u_{i+1}^n) \right)
 \end{aligned}$$

- Does not maintain monotonic solution
- Introduces dispersion errors as seen in linear advection example

Second Order



- A simple second order algorithm

$$\begin{aligned}u_i^{n+1} &= u_i^n + \frac{v\Delta t}{\Delta x} (F_{i-1/2} - F_{i+1/2}) \\&= u_i^n + \frac{v\Delta t}{\Delta x} \left(\frac{1}{2} (u_{i-1}^n - u_i^n) - \frac{1}{2} (u_i^n - u_{i+1}^n) \right)\end{aligned}$$

- Does not maintain monotonic solution
- Introduces dispersion errors as seen in linear advection example

Partial Interface Method

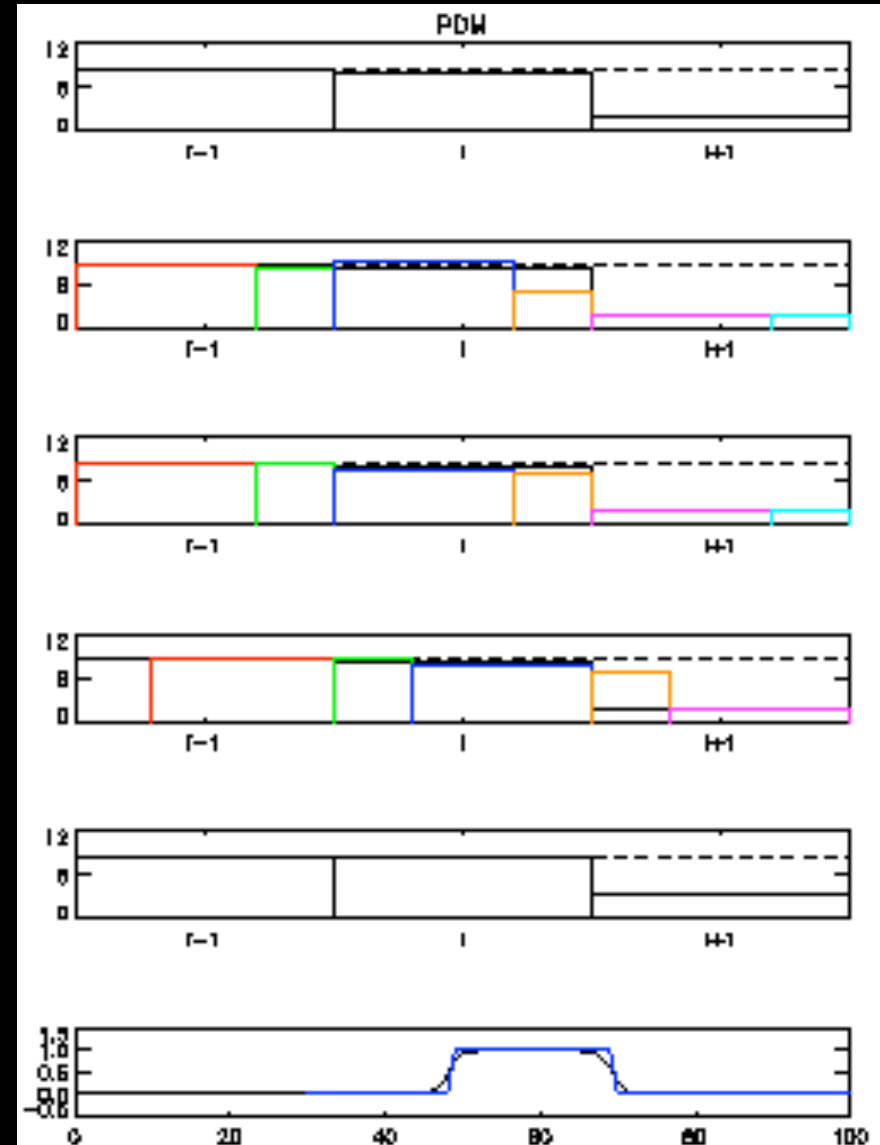
- Combines low order and high order fluxes

$$u_i^{n+1} = u_i^n + \frac{v\Delta t}{\Delta x} (F_{i-1/2} - F_{i+1/2})$$

$$F_{i+1/2} = \frac{1}{2} (u_i^n + u_{i+1}^n) + \frac{1}{2} \text{sign}(u_{i+1}^n - u_i^n) * \\ * \max(0, |u_{i+1}^n - u_i^n| - Bs_i |u_i^n - u_{i-1}^n|)$$

$$s_i = \frac{1}{2} |\text{sign}(u_{i+1}^n - u_i^n) + \text{sign}(u_i^n - u_{i-1}^n)|$$

- Limiter to keeps solution monotonic
- Provides nonlinear numeric resistivity and viscosity



Partial Interface Method

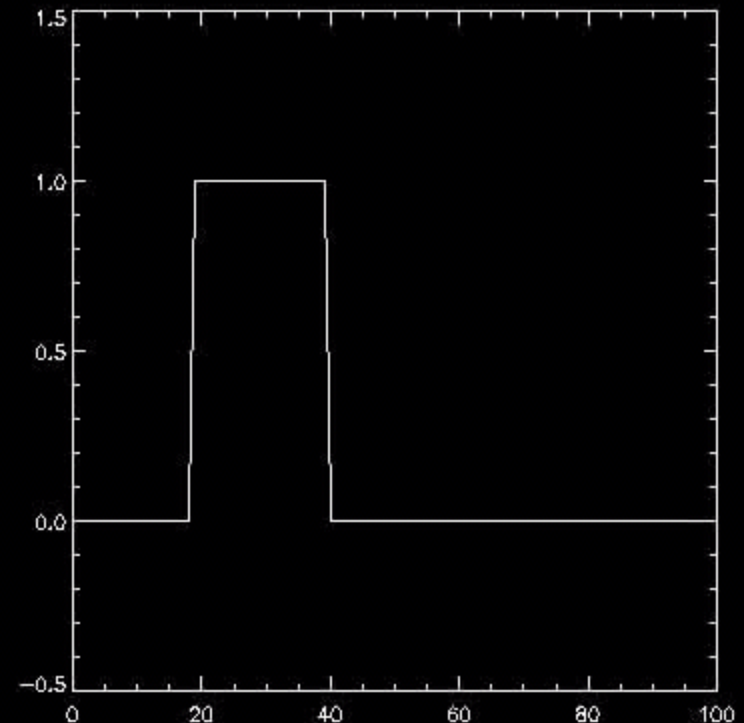
- Combines low order and high order fluxes

$$u_i^{n+1} = u_i^n + \frac{v\Delta t}{\Delta x} (F_{i-1/2} - F_{i+1/2})$$

$$F_{i+1/2} = \frac{1}{2} (u_i^n + u_{i+1}^n) + \frac{1}{2} \text{sign}(u_{i+1}^n - u_i^n) * \\ * \max(0, |u_{i+1}^n - u_i^n| - Bs_i |u_i^n - u_{i-1}^n|)$$

$$s_i = \frac{1}{2} |\text{sign}(u_{i+1}^n - u_i^n) + \text{sign}(u_i^n - u_{i-1}^n)|$$

- Limiter to keeps solution monotonic
- Provides nonlinear numeric resistivity and viscosity



Treatment of the Magnetic Field

- Various approaches can be used to satisfy the constraint that $\nabla \cdot \mathbf{B} = 0$

- Projection method

$$\nabla^2 \Psi = -\nabla \cdot \mathbf{B}$$

$$\mathbf{B}' = \mathbf{B} + \nabla \Psi$$

- $\nabla \cdot \mathbf{B}$ convection

- Modify the MHD equations so that $\nabla \cdot \mathbf{B}$ convects through the system

$$\frac{d(\nabla \cdot \mathbf{B})}{dt} = 0$$

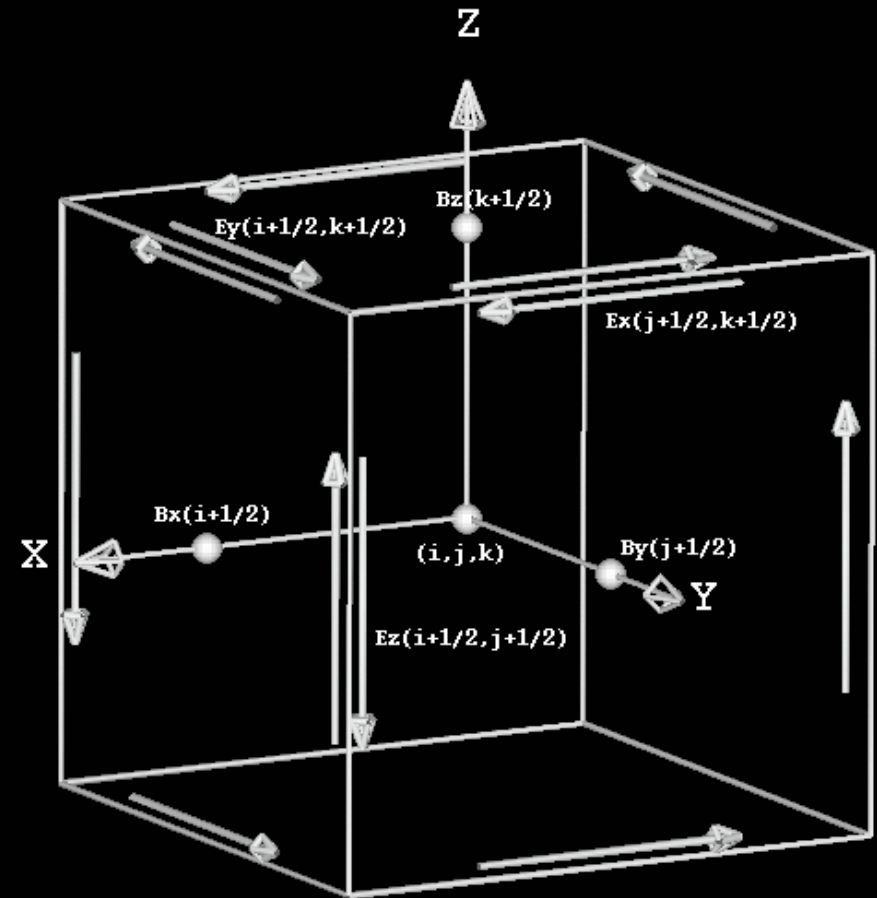
- Use a magnetic flux conservative scheme that keeps $\nabla \cdot \mathbf{B} = 0$

Magnetic Flux Conservative Scheme

- Magnetic field placed on center of cell faces
- Electric field is placed at center of cell edges so that

$$\frac{\partial}{\partial t}(B_x)_{i+\frac{1}{2},j,k} = \left[(E_y)_{i+\frac{1}{2},j,k+\frac{1}{2}} - (E_y)_{i+\frac{1}{2},j,k-\frac{1}{2}} \right] / \Delta z - \left[(E_z)_{i+\frac{1}{2},j+\frac{1}{2},k} - (E_z)_{i-\frac{1}{2},j+\frac{1}{2},k} \right] / \Delta y$$

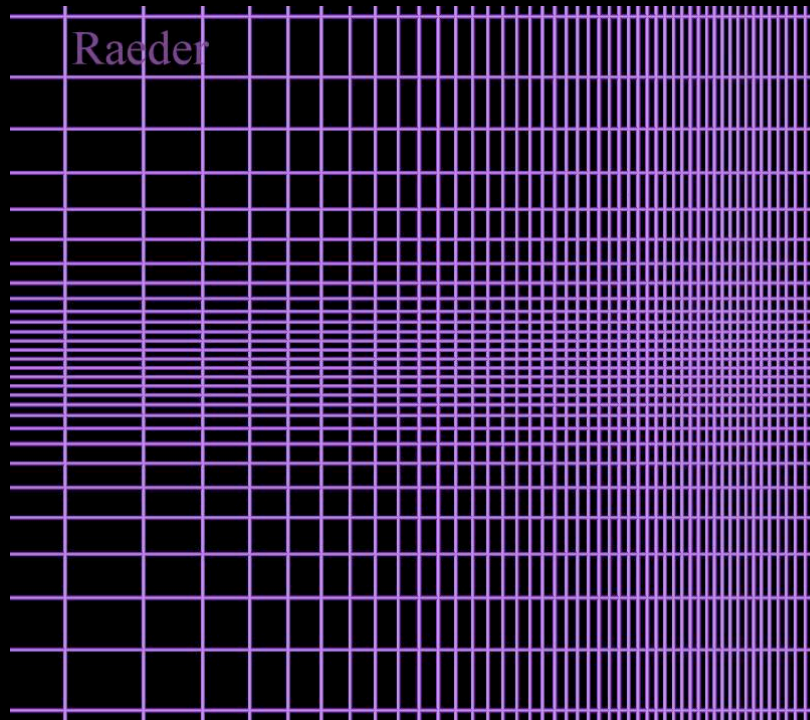
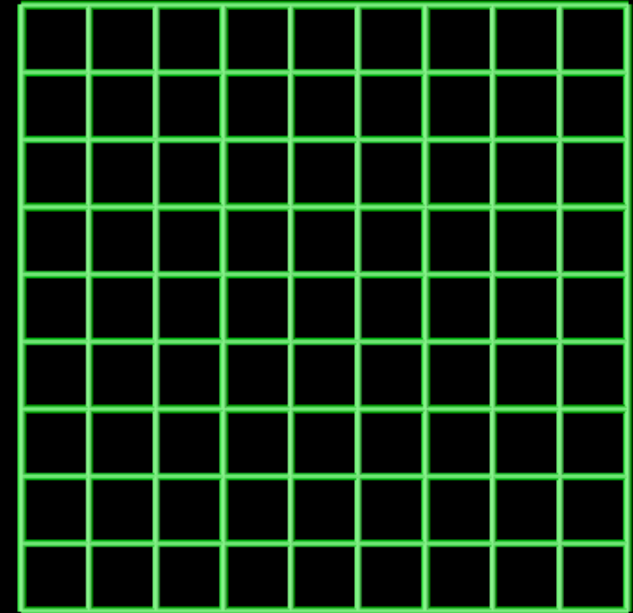
- Cancellation occurs when field components of all six faces are summed up



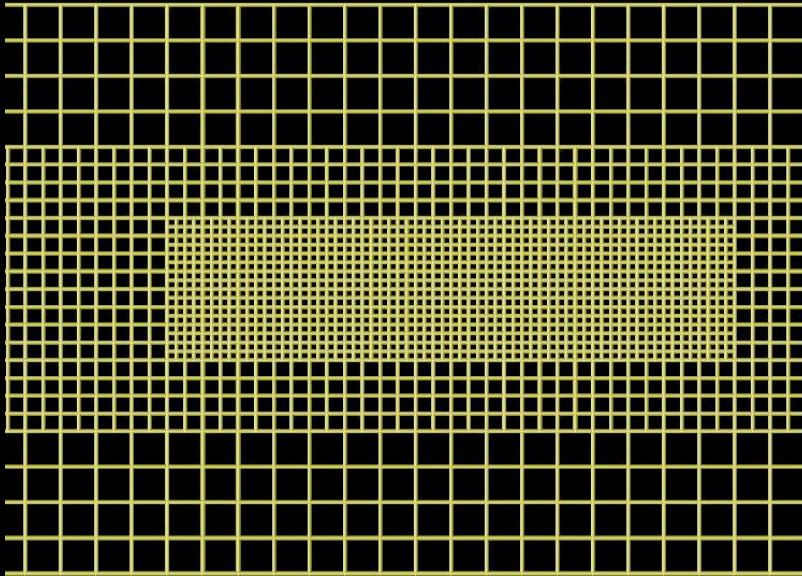
Computation Grids

- Simulation boundaries should be in supermagnetosonic flow regimes
 - $\geq 18 \text{ Re}$ from Earth on Sunward side
 - $\geq 200 \text{ Re}$ in tailward direction
 - $\geq 50 \text{ Re}$ in transverse directions
- A variety of grid types exist with varying degrees of complexity
 - Uniformed Cartesian
 - Stretched Cartesian
 - Nested Cartesian
 - Regular Noncartesian
 - Irregular Noncartesian

- Uniformed Cartesian Grid
 - Low programming overhead
 - Low computing overhead
 - No memory overhead
 - Easy parallelization
 - Not very adaptable

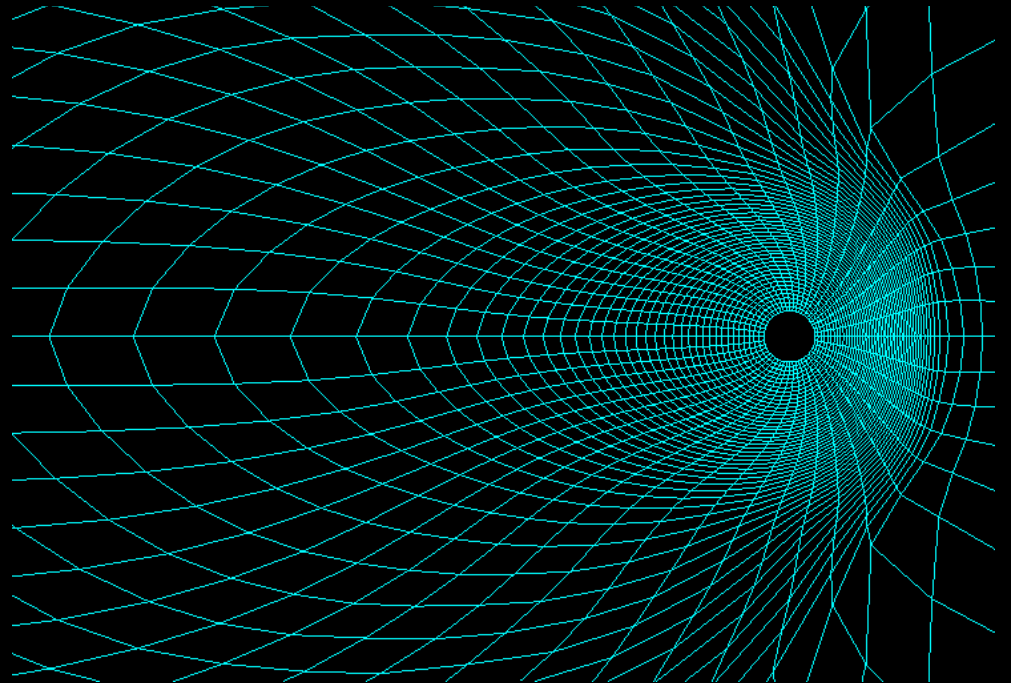


- Stretched Cartesian Grid
 - Low programming overhead
 - Low computing overhead
 - No memory overhead
 - Easy parallelization
 - Somewhat adaptable
 - Example from Raeder UCLA MHD Model

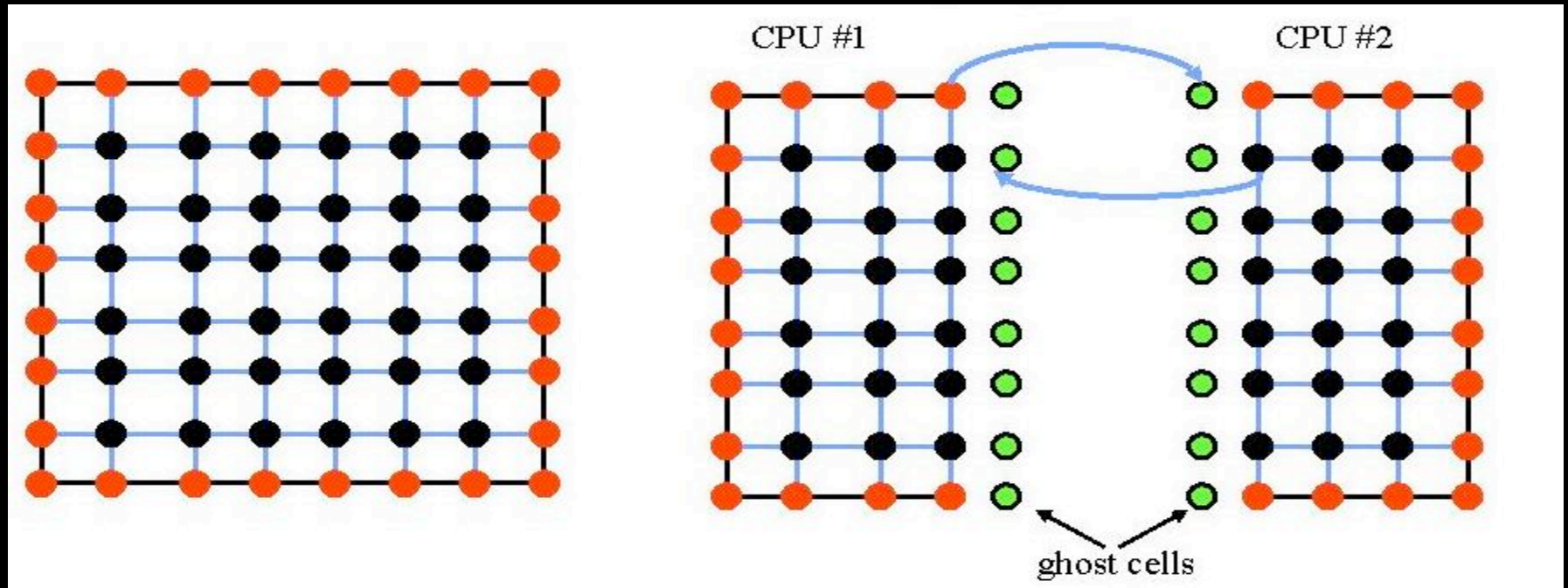


- Nested Cartesian
 - Medium/High programming overhead
 - Medium/High memory overhead
 - small computational overhead
 - difficult to parallelize
 - very (self) adaptable
 - Example from BATS-R-US

- Regular Noncartesian
 - Medium programming overhead
 - Low memory overhead
 - small computing overhead
 - parallelizes like regular cartesian grid
 - somewhat adaptable
 - Example from LFM



Domain Decomposition



- Computational Space is divided (evenly?) amongst the CPUs available to work on the problem
 - MPI used to pass boundary information between ghost cells at interfaces
 - Can also use packages like MultiBlockParti and P++

Boundary Conditions

- Upstream
 - Fixed or time dependent values for 8 plasma parameters
 - Can be idealized for derived from solar wind observations
 - Problem with B_x
 - Need to know 3D structure of solar wind because

$$\nabla \cdot \mathbf{B} = 0 \Leftrightarrow \mathbf{n} \cdot (B_{upstream} - B_{downstream}) = 0$$

- Implies $B_x = B_N$ cannot change if solar parameters are independent of Y and Z
- Find \mathbf{n} direction with no variation and then sweep these fronts across front boundary

Boundary Conditions II

- All other sides
 - Free flow conditions for plasma and transverse components of **B**

$$\frac{\partial \Psi}{\partial \mathbf{n}} = 0$$

- normal component of **B** flows from   **B**=0

- Inner Boundary Condition
 - MI Coupling module
 - Hard wall boundary condition for normal component of velocity and density

Magnetosphere-Ionosphere Coupling

- Inner boundary of MHD domain is placed between 2-4 R_E from the Earth
 - High Alfvén speeds in this region would impose strong limitations on global step size
 - Physical reasonable since MHD not the correct description of the physics occurring within this region
 - Covers the high latitude region of the ionosphere (45°-90°)
- Parameters in MHD region are mapped along static dipole field lines into the ionosphere
- Field aligned currents (FACs) and precipitation parameters are used to solve for ionospheric potential which is mapped back to inner boundary as boundary condition for flow

$$\mathbf{v} = \frac{(-\nabla\Phi) \times \mathbf{B}}{B^2}$$

Ionosphere Model

- 2D Electrostatic Model

- $\nabla \cdot (\epsilon_0 \nabla \phi) = J_{\parallel}$
- $\phi = 0$ at low latitude boundary of ionosphere

- Conductivity Models

- Solar EUV ionization
 - Creates day/night and winter/summer asymmetries

$$\Sigma_p = 0.5 F_{10.7}^{2/3} (\cos \chi)^{2/3} \quad \forall \quad \chi \leq 65^\circ$$

$$\Sigma_H = 1.8 F_{10.7}^{1/2} \cos \chi \quad \forall \quad \chi \leq 65^\circ$$

- Auroral Precipitation
 - Empirical determination of energetic electron precipitation

Auroral Precipitation Model

- Empirical relationships are used to convert MHD parameters into an average energy and flux of the precipitating electrons

- Initial flux and energy

$$\mathcal{E}_o = \alpha c_s^2 \quad \phi_o = \beta \rho \mathcal{E}_o^{1/2}$$

- Parallel Potential drops (Knight relationship)

$$\mathcal{E}_{||} = \frac{RJ_{||}\mathcal{E}_o^{1/2}}{\rho}$$

- Effects of geomagnetic field

$$\mathcal{E} = \mathcal{E}_o + \mathcal{E}_{||}$$

$$\phi = \phi_o \left(8 - 7e^{\frac{-\mathcal{E}_{||}}{7\mathcal{E}_o}} \right) \quad \forall \quad \mathcal{E}_{||} > 0$$

$$\phi = \phi_o e^{\frac{\mathcal{E}_{||}}{\mathcal{E}_o}} \quad \forall \quad \mathcal{E}_{||} < 0$$

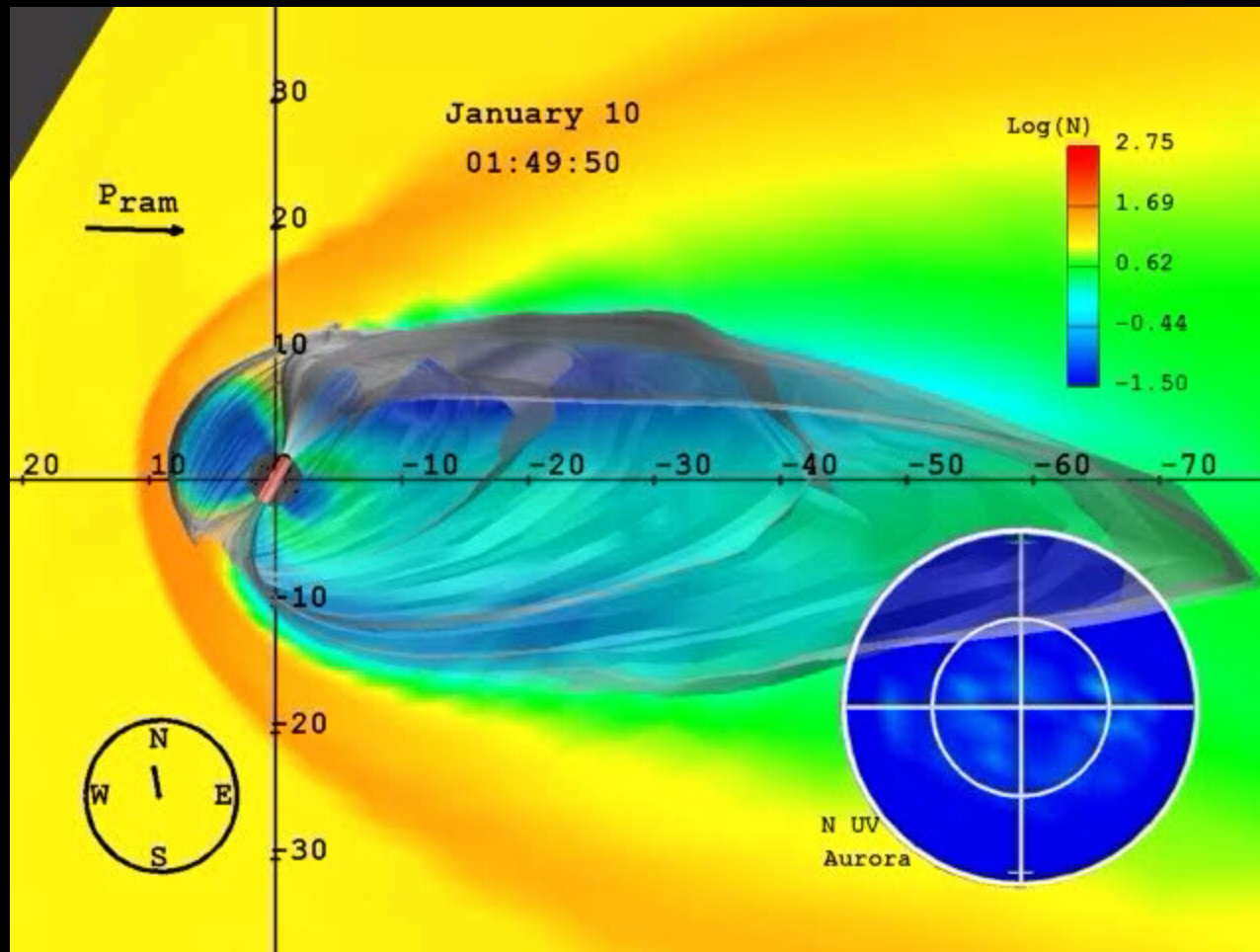
- Hall and Pederson Conductance from electron precp (Hardy)

$$\Sigma_p = \frac{5\mathcal{E}^{3/2}\phi^{1/2}}{(1 + 0.0625\mathcal{E}^2)}$$

$$\Sigma_H = 0.45\mathcal{E}^{0.85}\Sigma_p$$

Pretty Picture Time

- A whole lot of coding later and you get

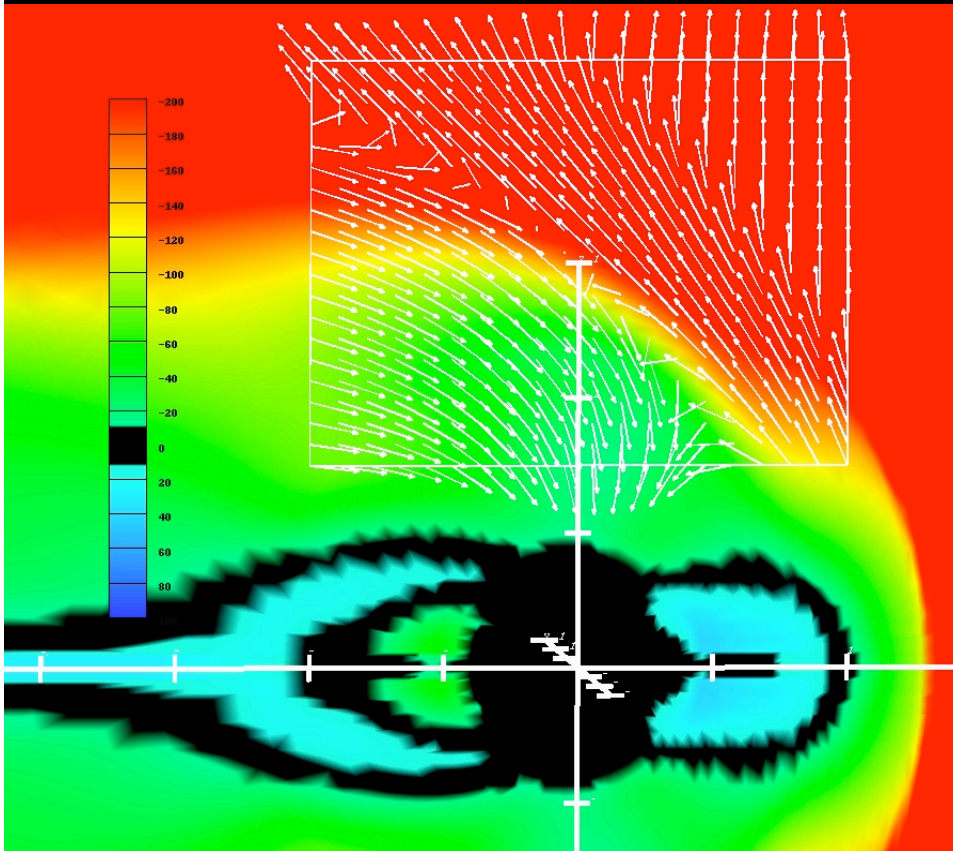


Methods of Model Validation

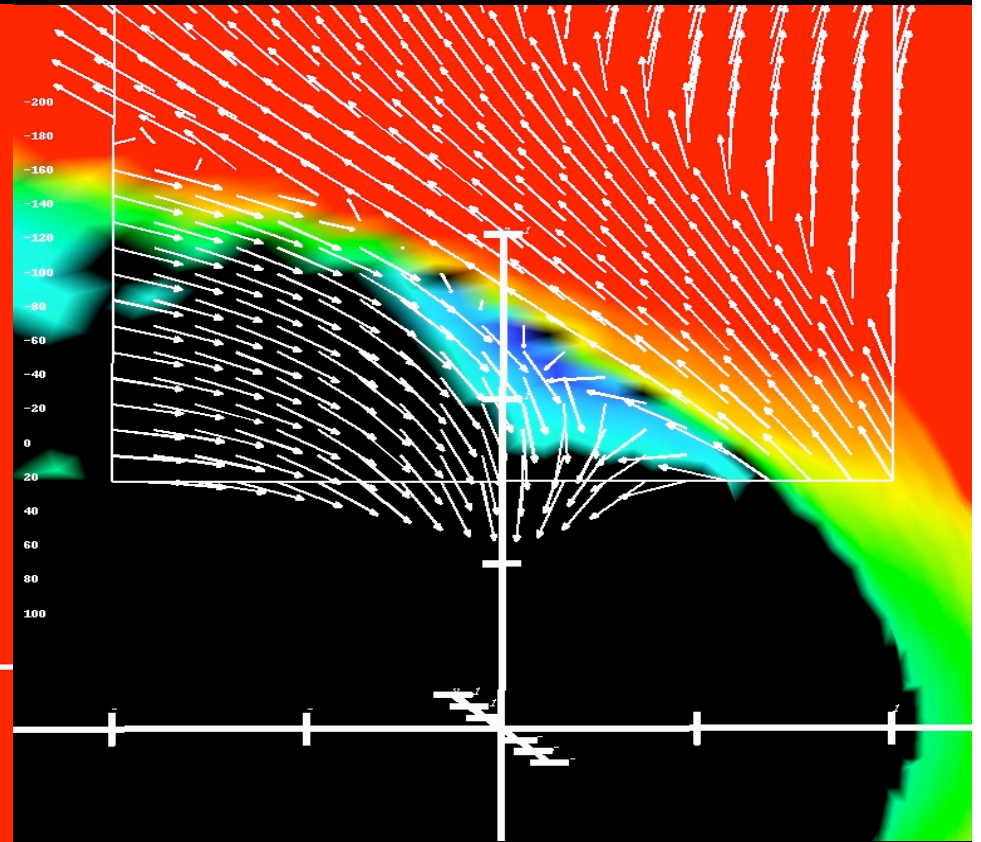
- Conduct studies with same conditions and different numerics
- Computation of theoretical problems with known analytic answers
 - Provides a ground truth that code is working
 - Very limited number of MHD problems
- Direct comparison with observations
 - Limited number of spacecraft observations
 - Check general characteristics with superposed epoch studies
 - Include comparison with indirect observations
 - Use metrics to quantitatively assess validity

Effect of Numerics on Magnetosphere

- Simulation for Northward IMF with constant Pedersen Conductance
 - Background color velocity with white magnetic field vectors



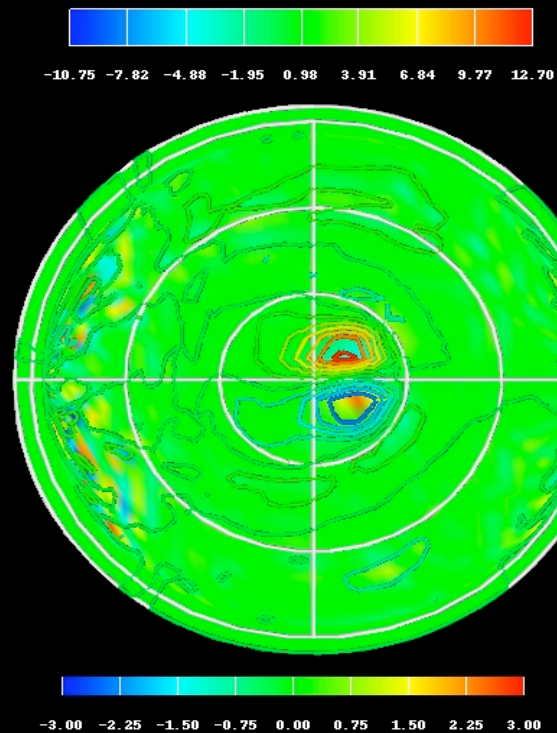
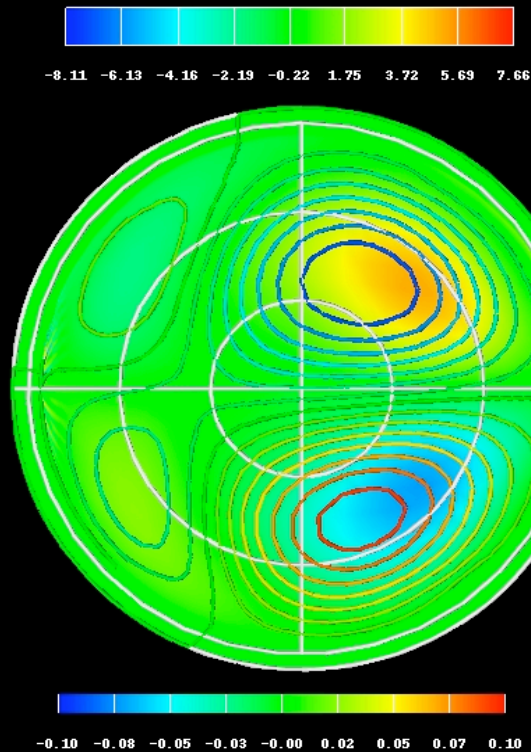
- High Numerical Diffusion
 - 8th Order
 - No TVD Scheme



- Low Numerical Diffusion
 - 8th Order
 - High TVD Scheme

Effect of Numerics on Ionosphere

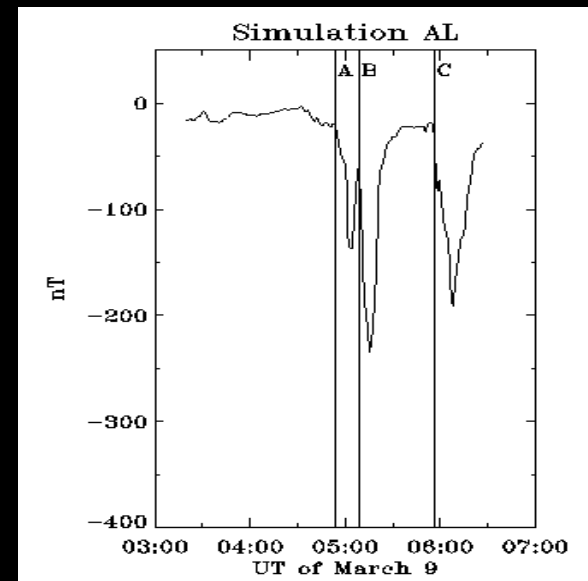
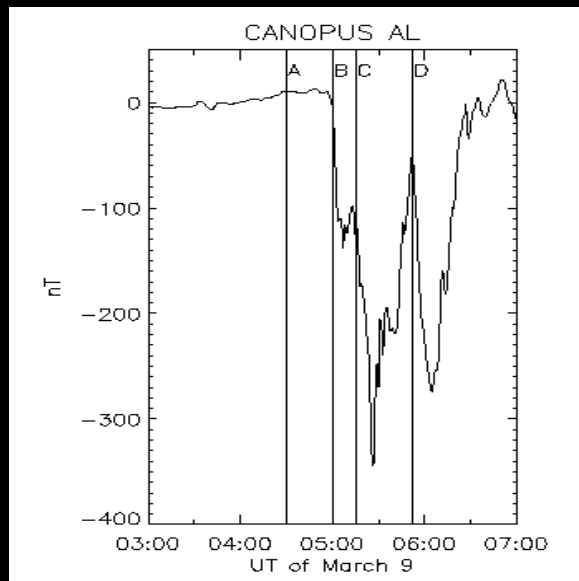
- Simulation for Northward IMF with constant Pedersen Conductance
 - Background color FAC strength with potential contours overlaid



- High Numerical Diffusion
 - 8th Order
 - No TVD Scheme

- Low Numerical Diffusion
 - 8th Order
 - High TVD Scheme

Energy loading and unloading

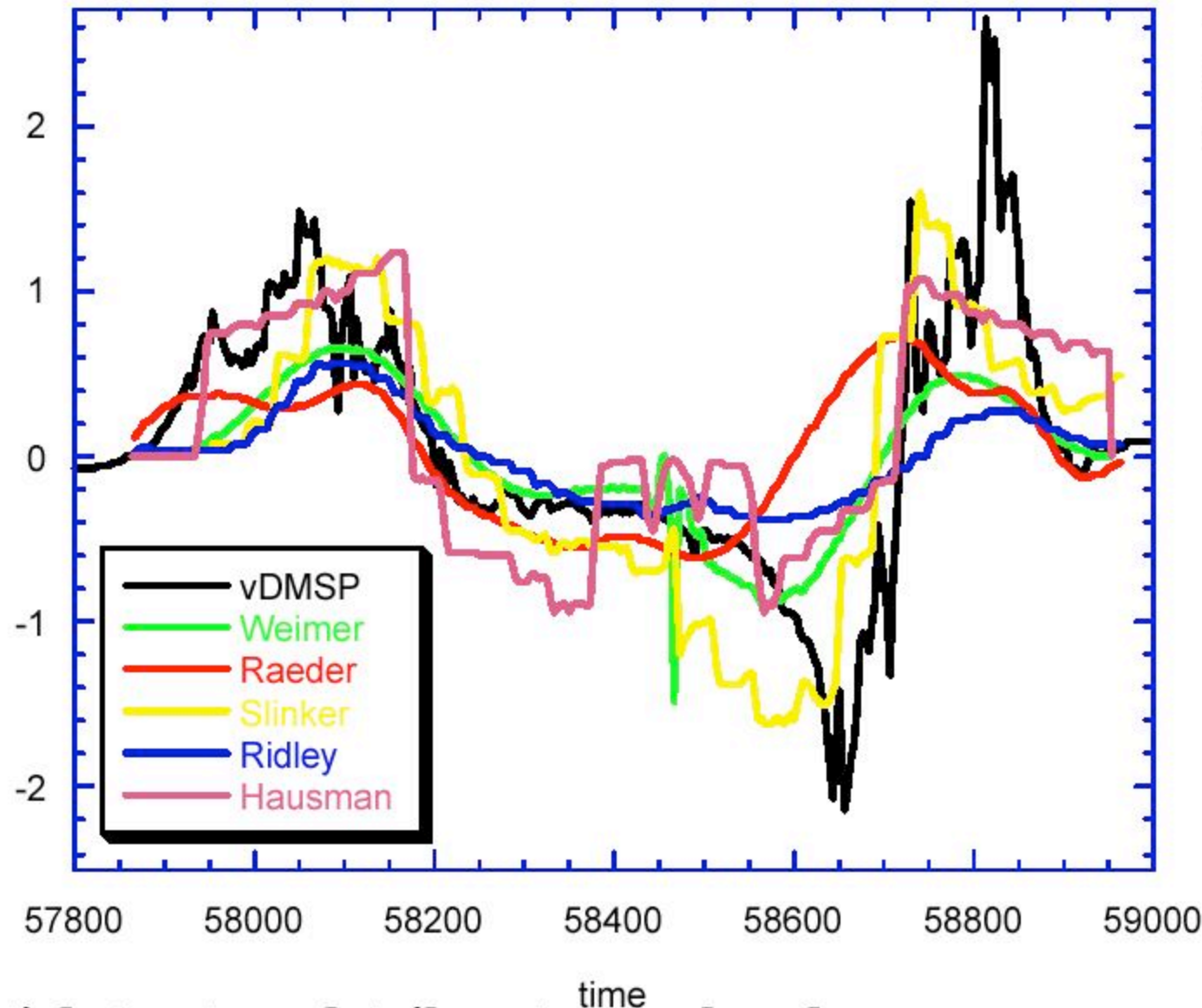


- Both data and simulation show onset, intensification, recovery, and second onset
- Simulated onset is early, but intervals between intensification and second onset are consistent
- Simulated CL recovers faster than observations

Medium Skill Case 1

DMSF data-model comparison
a1398310.154

Raeder: 0.27
Ridley: 0.32
Rice: 0.32
Slinker: 0.23
Weimer: 0.43

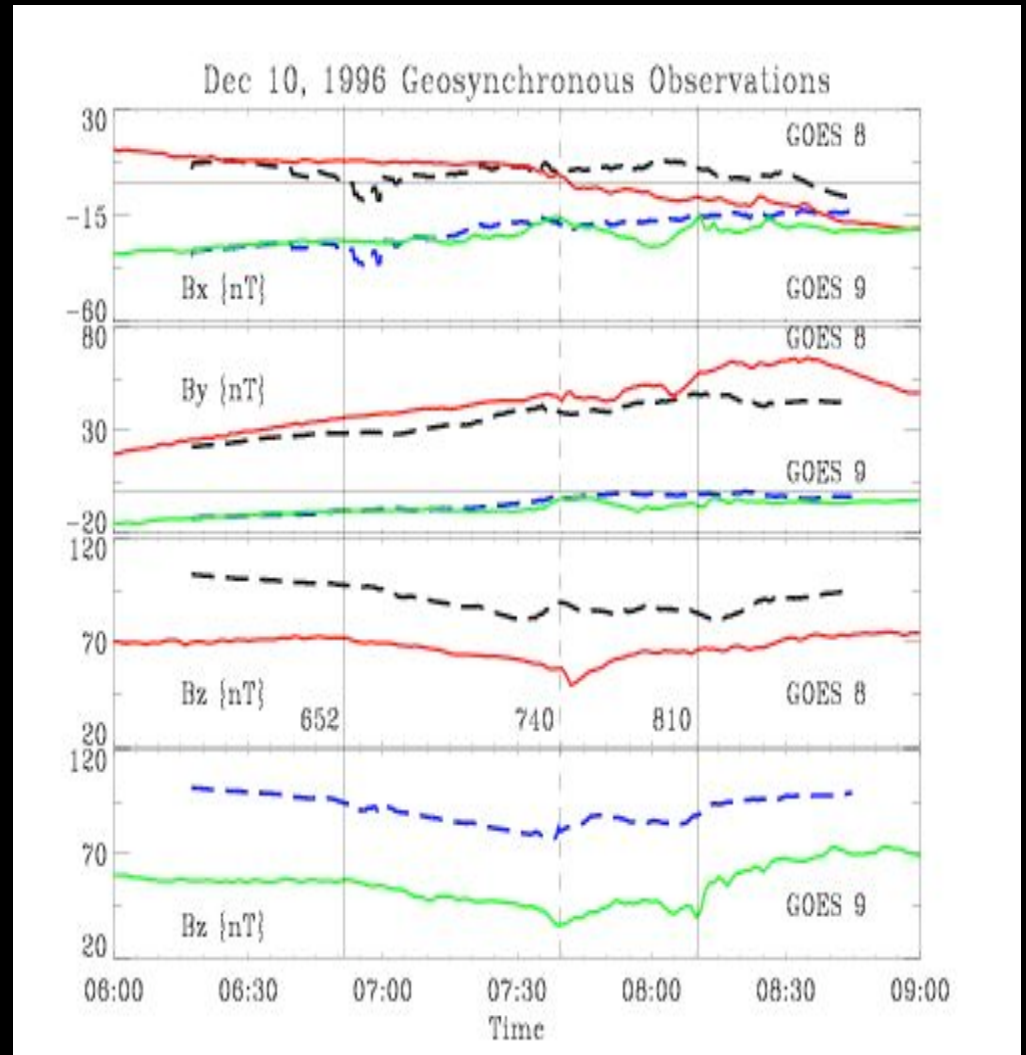


Spatial structure details not reproduced

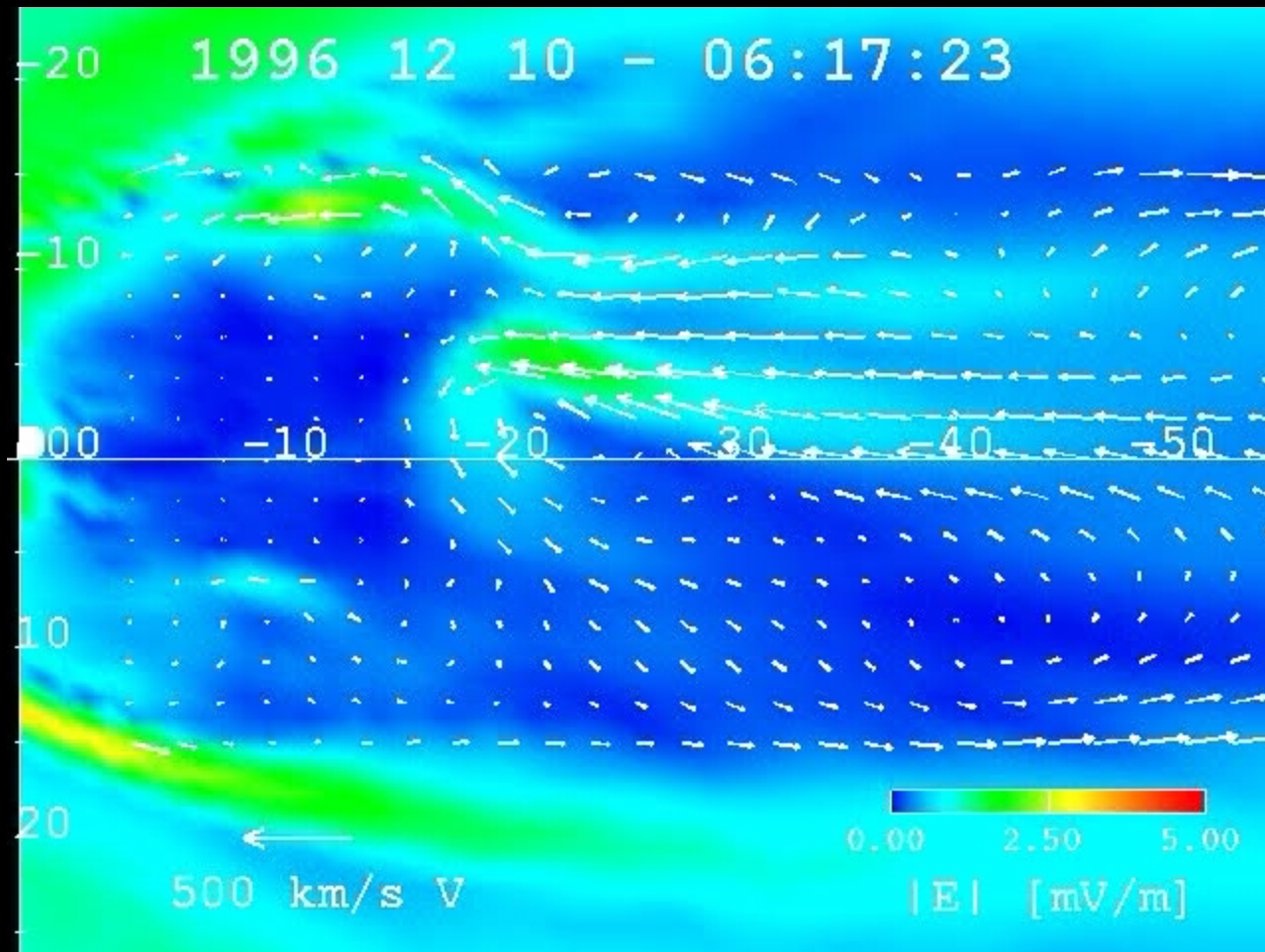
**More detail (Rice, Slinker) does not necessarily lead to higher skill,
although it is desirable**

Comparison with geostationary observations

- Excellent agreement for all three components of B
- Despite global B_z offset dipolarizations of similar size are seen in simulation results for both GOES 8 & 9
 - May imply limited role for ring current in substorms

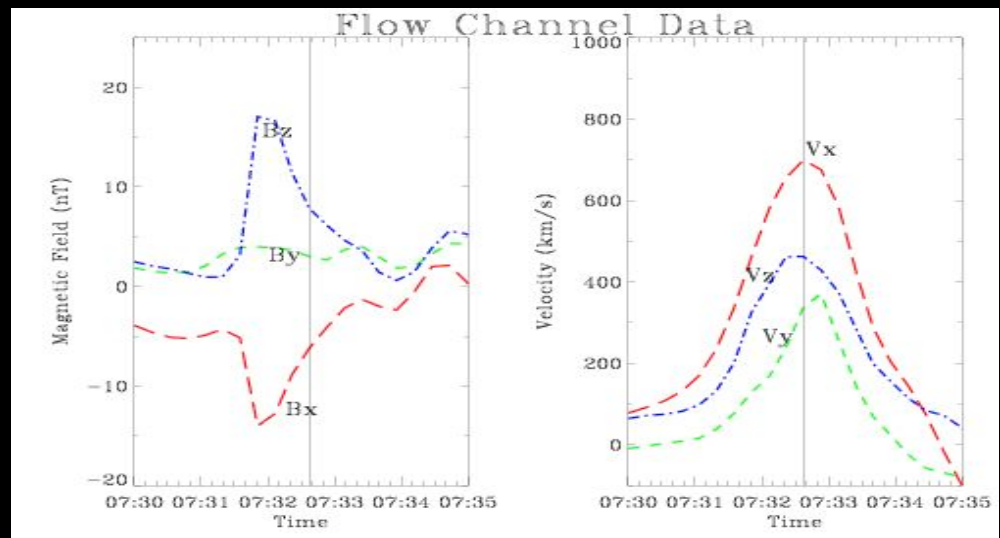
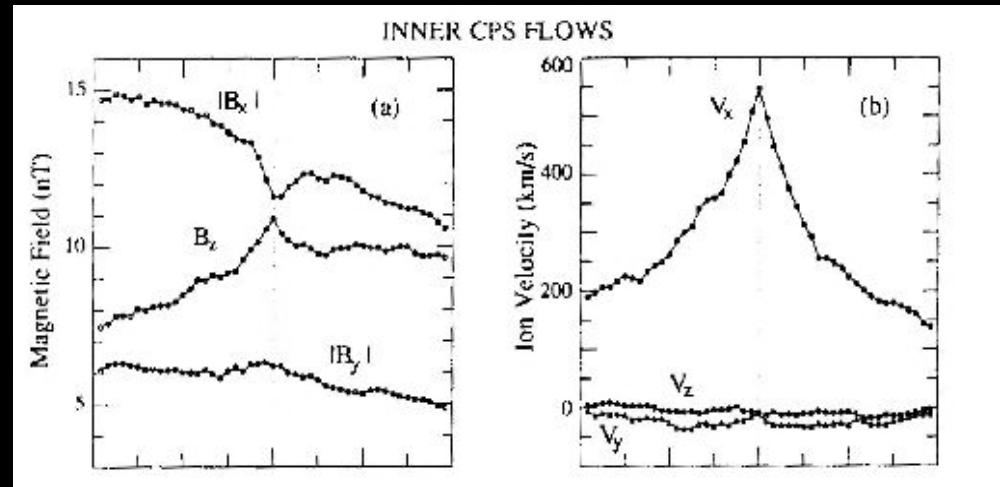


Flow Channels



Comparison between Flow channels and BBFs

- Flow channels have properties similar to BBF results reported by Angelopoulos
- FWHM of V_x profile and magnitude comparable BBF properties
- Use code to determine if they result from localized reconnection or interchange instability



LFM-TING Coupling

Solar Wind

LFM Model

$\Phi, T, j_{||}$

$E = -\nabla \Phi$

*Coordinate transfer
Data interpolation*

Magnetosphere-Ionosphere Coupler

Particle precipitation: F_e, E_0

$\Phi, T, j_{||}, J_{||}$

Electric potential: Φ

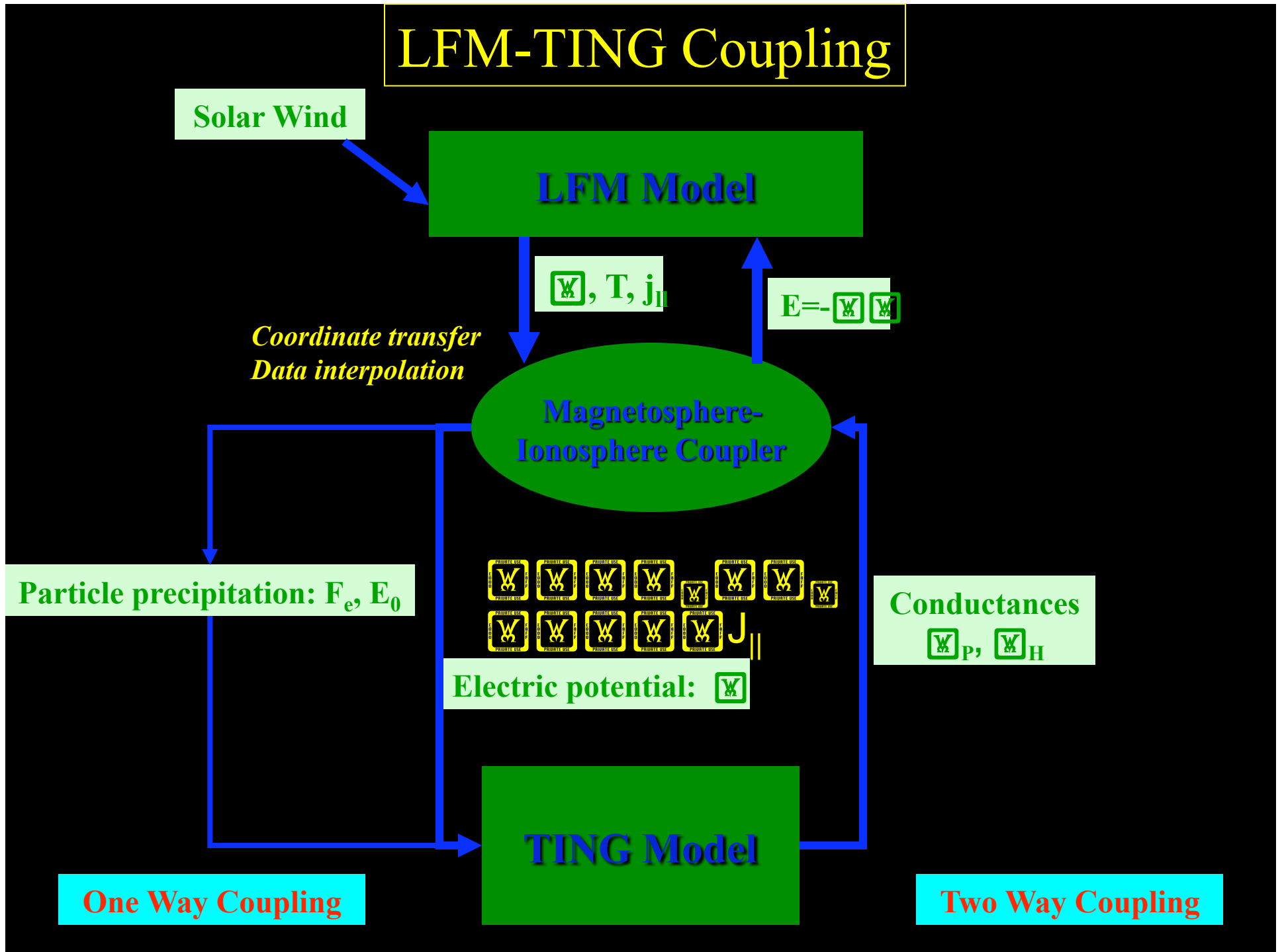
Conductances

Σ_P, Σ_H

TING Model

One Way Coupling

Two Way Coupling



Conclusions

- Global MHD simulation of the magnetosphere under idealized solar wind conditions are proving to be a useful tool for expanding our understanding the coupled solar wind – magnetosphere – ionosphere system
- The technique is expanding into new frontiers
 - Ionospheric simulation is being replaced with more sophisticated Thermosphere-Ionosphere Global Circulation Models
 - Modeling of the inner magnetosphere is being enhanced by coupling with the Rice Convection Model

Conclusions

- LFM is highly successful global MHD simulation of the magnetosphere
 - Numerous publications and presentations
 - Its design considerations are still relevant today
- LFM is still evolving
 - Ports to new platforms and utilization of MPI
 - Ionospheric simulation is being replaced with more sophisticated Thermosphere-Ionosphere Global Circulation Models
 - Modeling of the inner magnetosphere is being enhanced by coupling with the Rice Convection Model